Chemical Engineering Journal 370 (2019) 573–586

Contents lists available at ScienceDirect

Chemical Engineering Journal

journal homepage: www.elsevier.com/locate/cej

Synergistic effect of stem cells from human exfoliated deciduous teeth and rhBMP-2 delivered by injectable nanofibrous microspheres with different surface modifications on vascularized bone regeneration

Tengjiaozi Fang[a], Zuoying Yuan[b], Yuming Zhao[a], Xiaoxia Li[a], Yue Zhai[a], Jingzhi Li[a], Xiaotong Wang[a], Nanquan Rao[a], Lihong Ge[a,*], Qing Cai[b,*]

[a] Department of Pediatric Dentistry, Peking University School and Hospital of Stomatology, National Engineering Laboratory for Digital and Material Technology of Stomatology, and Beijing Key Laboratory of Digital Stomatology, Beijing 100081, China
[b] State Key Laboratory of Organic-Inorganic Composites, Beijing Laboratory of Biomedical Materials, Beijing University of Chemical Technology, Beijing 100029, China

HIGHLIGHTS

- We applied different surface modifications on-demand to injectable NF-Ms.
- Bio-inspired hydrophilic modification by PDA supported the cellular behavior.
- Hep-Dopa conjugation improved performance of NF-Ms in loading and delivering rhBMP-2.
- SHED engraftment contributes to angiogenesis in ectopic and orthotopic sites.
- Conjunctive use of SHED and rhBMP-2 led to vascularized bone tissue regeneration.

GRAPHICAL ABSTRACT

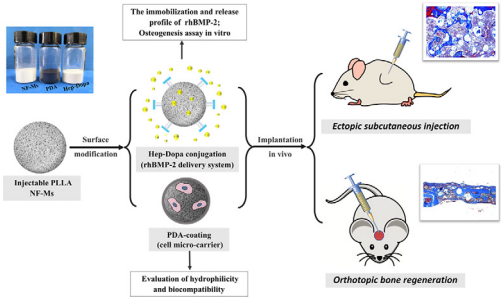

ARTICLE INFO

Keywords:
Injectable nanofibrous microspheres
Surface modification
Stem cells from human exfoliated deciduous teeth
Cell micro-carrier
Sustained release system

ABSTRACT

To provide a suitable 3D microenvironment for bone regeneration, we selected the injectable poly (l-lactic acid) nanofibrous microspheres (PLLA NF-Ms) with different surface modifications to serve as cell micro-carriers or protein vehicles on-demand. Results showed that polydopamine (PDA) modified NF-Ms (PDA-NF-Ms) exhibited good affinity for stem cells from human exfoliated deciduous teeth (SHED), and Heparin-Dopamine (Hep-Dopa) conjugated with NF-Ms (Hep-Dopa NF-Ms) are able to immobilize and slowly release recombinant human bone morphogenic protein-2 (rhBMP-2) efficiently. In vivo evaluations were carried out in both ectopic subcutaneous implantation and orthotopic cranial bone defect nude mouse models (φ = 4 mm). The results suggested that PDA-NF-Ms could support SHED survival over 4 weeks. All experimental groups with SHED/PDA-NF-Ms engraftment showed angiogenesis activity. But, no effect of SHED/PDA-NF-Ms on osteogenesis was found in ectopic implantation, which is different from the result in cranial defect. The rhBMP-2 released from Hep-Dopa NF-Ms could significantly guide bone tissue regeneration in both ectopic and orthotopic site. At 8 weeks, both BMP-2 group and dual group showed large amounts of bone formation in situ, despite the fact that quantitative results of micro-CT did not demonstrate significant difference between them. More blood vessels were observed in SHED and Dual groups, which verifies the quality improvement of regenerated osseous tissues. Regeneration of vascularized bone tissue was, thus, highly expected upon implanting SHED/PDA-NF-Ms and rhBMP-2-loaded

* Corresponding authors.
E-mail addresses: gelihong0919@163.com (L. Ge), caiqing@mail.buct.edu.cn (Q. Cai).

https://doi.org/10.1016/j.cej.2019.03.151
Received 21 October 2018; Received in revised form 14 March 2019; Accepted 16 March 2019
Available online 20 March 2019

Hep-Dopa NF-Ms together. The strategy developed in this study represents a promising method for satisfactorily promoting bone regeneration.

1. Introduction

Critical bone defects are generally caused by maxillofacial tumors, periodontitis, and congenital skeletal deformities, among other conditions. The treatment of these defect is necessary to recover bone structure and function, which is a still a challenge worldwide. Tissue engineering, as a novel strategy for bone reconstruction, has overcome many disadvantages of conventional autologous bone grafting, such as limited bone sources, surgical trauma, and infection risks [1,2].

Tissue engineering often involves the use of stem cells which are cultured on the surface of scaffolds and induced to generate new bone tissue by osteoinductive molecules [3]. Nevertheless, there is mounting evidences indicates a predominant paracrine trophic role of stem cells in promoting tissue regeneration due to their enriched secretome in production of angiogenic and chemotactic factors, rather than their direct replacement of damaged cells at the injury site [4]. Given that, it is necessary to improve the microenvironment of bone damage and mobilize progenitor cells for better healing outcomes. Stem cells from human exfoliated deciduous teeth (SHED), which originate from the neural crest and expressing mesenchymal stem cell markers, have recently gained more attention than bone marrow-derived stem cells (BMSCs) in regenerative medicine currently. Compared with BMSCs, SHED can be obtained noninvasively, and their ability of extensive proliferation and multiple differentiation capabilities are more prominent [5–7]. Besides, SHED have shown the multifaceted therapeutic functions on many disease models, which can be attributed to their paracrine effects on anti-inflammation, pro-angiogenesis, and anti-apoptosis effects [8–10]. However, the inductive effect of SHED on osteogenesis and a suitable scaffold for their implantation in vivo have been rarely reported.

Advanced tissue engineering scaffolds should have good biodegradability and biocompatibility; possess a nanoscale or macroscale structure that is similar to native bone architecture; and mimic the microenvironment to support cell migration, proliferation, and oriented differentiation [11]. In comparison with traditional pre-formed scaffolds, injectable microspheres can be applied in a minimally invasive manner to easily fill and repair irregularly shaped tissue defects via direct injection, which decreases the risk of infection from a surgical procedure [12,13]. Due to the huge specific surface area and extracellular matrix (ECM)-like structure of nanofibers, injectable microspheres, especially those with nanofibrous architecture, are suitable to serve as cell micro-carriers to facilitate cell-material interactions [14]. Previous studies showed the ideal properties of PLLA nanofibrous microspheres to deliver dental pulp stem cells (DPSCs) and promote dentin-pulp tissue regeneration [15]. However, such synthetic scaffold materials are 'bio-inert', and therefore cannot effectively recruit endogenous stem cells to migrate onto the scaffold [14]. At present, dopaminergic surface modification has been widely applied to improve the hydrophilicity of materials, providing a beneficial microenvironment for cell adhesion and migration without causing adverse effects on cell biological behaviors [16]. Based on this information, we supposed that coating PLLA nanofibrous microspheres (NF-Ms) with polydopamine (PDA) could improve its biological properties to act as an appropriate micro-carrier for SHED.

As an extensively studied recombinant growth factor, bone morphogenetic protein-2 (BMP-2) has been successfully applied for treating bone diseases or inducing osteogenesis in endogenous cells [17,18]. There have been plenty of attempts to develop an effective carrier for delivering BMP-2 into a defective area while considering its spatiotemporal distribution and optimal dosage to avoid complications and rapid diffusion [19]. Although the PDA-assisted coating strategy has also been applied to modify scaffolds for protein delivery [20], the high affinity of Heparin to form covalent bonds with proteins makes it more effective as a sustained delivery system while maintaining proteins bioactivity [21]. Kim et al. prepared BMP-2-immobilized porous microspheres modified with Hep-Dopa, which provided optimal

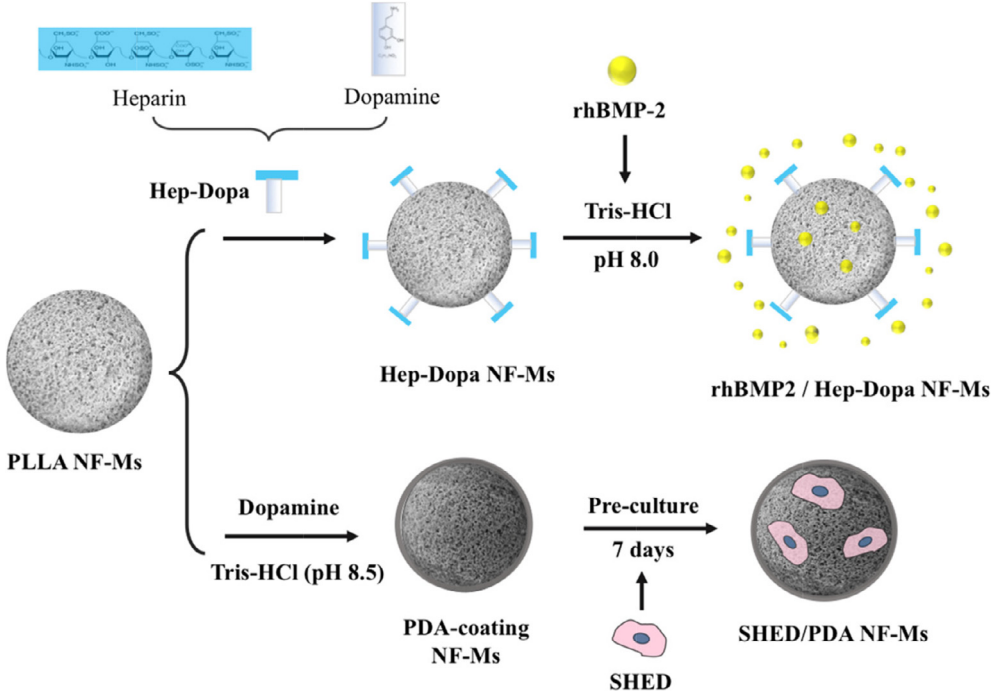

Scheme 1. Schematic illustration for synthesis of NF-Ms with different surface modifications.

conditions for the long-lasting release of BMP-2 to induce osteogenic differentiation of cells [22]. Nevertheless, the small size of nanofibrous structures has advantages over porous structures, which can provide more binding sites for proteins [16]. Herein, we functionalized the surface of PLLA NF-MS by Hep-Dopa conjugation to immobilize BMP-2 and promote its controlled release and evaluated the effectiveness of this novel protein delivery system for bone tissue engineering.

Multiple polymer scaffolds modified via single surface-modification strategies have been developed to improve the delivery of stem cells and biomolecules. However, most of these tissue engineering scaffold are non-specific delivery systems, which cannot efficiently satisfy the needs of both. Hence, the objective of this study was to design a bioactive PLLA NF-MS scaffold that modified with either a PDA layer or Hep-Dopa, which further specifically targeted SHED to support their long-time survival and deliver BMP-2 constantly to enhance bone tissue regeneration. We suppose that the involvement of SHED may promote bone tissue regeneration more than a single application of BMP-2, which is not only achieved by the paracrine trophic effect of SHED to improve the microenvironment, but also resulted from the synergistic effect of their combination.

2. Materials and method

2.1. Preparation of microspheres

Nanofibrous microspheres (NF-Ms) were fabricated via a phase separation method as previously described [23]. Briefly, 1 g PLLA (MW = 50,000, Shandong College of Pharmacy, China) was dissolved in 50 ml tetrahydrofuran (THF) at a concentration of 2.0% (wt/v) at 50 °C and the solution was rigorously agitated to ensure adequate dissolution. Afterwards, heated glycerol was gradually poured into the PLLA solution at a ratio of 3:1 under mechanical stirring for 10 min. This mixture was then quickly poured into liquid nitrogen and added into a water/ice mixture for 24 h to promote solvent exchange. To ensure that the glycerol residue was removed, NF-Ms washed with distilled water every 3 h. Then, PLLA NF-Ms were lyophilized for 48 h and stored at room temperature for further use.

2.2. Modification of NF-MS with PDA and Hep-Dopa

We modified injectable NF-Ms with either PDA-coating or Hep-Dopa conjugation for different purpose. The schematic diagram clearly shows the synthesis process of two kinds modification (see Scheme 1). For coating with PDA, NF-Ms were directly soaked into a dopamine (DA) (Sigma–Aldrich) solution (2 mg/mL in 10 mM Tris-HCl, pH 8.5) and evenly stirred for 24 h at room temperature. The obtained PDA-NF-Ms were rinsed with deionized water (DI) water for several times to ensure that the ions and adsorbed polymers were removed completely; this was followed by freeze-drying overnight.

To functionalize and immobilize heparin on the surface of NF-Ms, heparin was first chemically conjugated with dopamine. Briefly, 400 mg heparin was reacted with 190.4 mg EDC (Thermal Scientific, USA) and 114.8 mg NHS (Sigma, USA) in 10 ml of MES buffer (pH 4.5) and allowed to react for 10 min. Then, DA (102.2 mg) dissolved in 1 ml of MES (pH 4.5) was added to the activated heparin solution and allowed to react overnight. The mixture was dialyzed (molecular weight cutoff (MWCO) = 2000, Spectrum®) against acidified distilled water for 48 h and lyophilized at last. Then, 2 mg/ml Hep-Dopa was dissolved in 10 mM Tris-HCl (pH 8.0). NF-Ms were added to the Hep-Dopa solution, and this reaction was maintained overnight in the dark environment. The resultant Hep-Dopa NF-Ms were washed with DI water and dried under nitrogen. All microspheres used in this study were sterilized by exposure to ultraviolet light for 6 h.

2.3. Characterization of NF-Ms and modified NF-Ms

The surface morphology and microstructure of NF-Ms, PDA-NF-Ms and Hep-Dopa NF-Ms were characterized by a scanning electron microscope (SEM, Hitachi, S-2400. Japan). Each specimen was dehydrated and immobilized on the surface of an aluminum stub via a double-sided adhesive carbon tape, then sputtered with gold (vacuum, 20 mA, 120 s) using a sputter-coater (Polaron E5600, USA) and observed by utilizing SEM at an accelerating voltage of 10 kV. The size distribution of the microspheres was determined by analyzing the SEM images with Nano Measurer (V1.2.5) Software. The elemental analysis was performed by energy dispersive spectroscopy (EDS) and elemental mapping (under 15 KV as SEM observation with an exposure time of 180 s). The hydrophilicity of various microspheres was evaluated by testing the water contact angle (WCA). PLLA NF-Ms, PDA-NF-Ms, and Hep-Dopa NF-Ms were pressed into similar plate-like samples to estimate the effect of the surface components on hydrophilicity.

2.4. BMP-2 immobilization and release assay

To impregnate rhBMP-2 on NF-Ms, a 500 ng/ml rhBMP-2 solution (stabilized by BSA) was added to the Hep-Dopa modified NF-Ms (mass ratio of BMP-2/polymer = 10 ug/mg) in 0.1 M MES buffer (pH 5.6). Then, this mixture was shaken overnight to fix positively charged rhBMP-2 on Hep-Dopa NF-Ms by using a magnetic stirrer (JOANLAB HS-17) at 150 rpm. NF-Ms without any modification were loaded with rhBMP-2 via the same approach as the control. The encapsulation efficiency of immobilized rhBMP-2 was determined as the difference in values of the original rhBMP-2 solution and in the supernatant by an enzyme-linked immunosorbent assay (ELISA) kit (Abcam, MA). Next, two kinds of NF-Ms were washed with DI water to remove free rhBMP-2 and lyophilized [24]. The obtained rhBMP-2-loaded microspheres were lyophilized and stored at −80 °C for later experiments.

To visualize the distribution of rhBMP-2 in microspheres with or without Hep-Dopa conjugation, the RBITC-labelled rhBMP-2 (PeproTech, USA) was applied according to the procedure described above. Briefly, two kinds of microspheres were mixed with RBITC-labelled rhBMP-2 (at a concentration of 500 ng/ml) in MES buffer (pH = 5.6), and incubated for 3 h at room temperature in the dark. Thereafter, the samples were washed with phosphate buffered saline (PBS, pH = 7.4) for three times to remove unbound fluorescent dyes before imaging through laser scanning confocal microscopy (LSCM, Nikon, Japan).

For the release study, rhBMP-2-loaded NF-Ms with or without Hep-Dopa conjugation were immersed in 5 ml PBS (pH 7.4) at 37 °C under continuous shaking. The in vitro release kinetics of proteins released from two kinds of microspheres was examined on days 1, 3, 5, 7, 10, 14, 21, and 28. At specific time intervals, 1 ml supernatant was collected and replaced with an equal amount of fresh PBS for 4 weeks. The quantity of rhBMP-2 released from microspheres was measured by using a rhBMP-2 ELISA Kit (n = 5).

2.5. Cell culture

Normal exfoliated human deciduous teeth and human bone marrow stromal cells (BMSCs) were a gift from the Oral Stem Cell Bank (China, Beijing). These cells were characterized by this public institution and stored in liquid nitrogen vapor for long-term cryopreservation. Briefly, after SHEDs and BMSCs were thawed, they were incubated in α-MEM (Life Technologies, CA, US) supplemented with 10% fetal bovine serum (FBS, Gibico, USA) and 1% penicillin-streptomycin (100 U/ml and 100 μg/ml, Invitrogen, UK) in an atmosphere containing 5% CO_2 and 95% O_2 at 37 °C. Both SHED and BMSCs were passaged when confluence reached 80% and cells were used after three to five passages.

2.6. The biological effects of PDA-NF-Ms on SHED

Before being applied for in vitro cell culture, all the prepared microspheres were soaked in 75% ethanol for 1 h to pre-wet the surface, then washed with PBS three times to replace the residual ethanol. Then, the microspheres were immersed in a α-medium with serum overnight to aid cell attachment. On the next day, SHED were seeded at a density of 1×10^6 cells/ml onto the 0.5 mg (about 1×10^5 spheres) of PDA-NF-Ms (10:1 ratio) and co-cultured for at least 4 h to promote cell attachment. The obtained SHED/PDA-NF-Ms constructs were further used in all in vitro and in vivo experiments.

Cells adherence and spreading on PLLA NF-Ms and PDA-NF-Ms were observed by SEM. After SHED were seeded onto microspheres and co-cultured for 7 days, the constructs were retrieved and fixed with 4% paraformaldehyde. For morphological characterization of SHED, the samples were dehydrated rapidly by using a serious of graded ethanol solutions. Then, the dried mixture was further viewed by SEM as previously described.

The viability of SHED on the surface of NF-Ms was assessed by a live/dead assay kit (Invitrogen, USA) at 7 days after cell seeding. Briefly, the SHED/PDA-NF-Ms were rinsed with PBS three times and then incubated with a PBS solution containing 2 μM calcein AM and 4 μM ethidium homodimer-1 for 30 min at room temperature. The constructs were then washed with PBS several times, and the viable cells emitting green fluorescence (dead cells were red-labelled) were observed by LSCM.

Immunofluorescent staining was performed to characterize the morphology of the cells that attached to microspheres. After the cells were fixed on NF-Ms and PDA-NF-Ms, the construct was then permeabilized with 0.1% Triton X-100 for 10 min and blocked with 1% BSA for 1 h. Afterwards, the cells and microspheres were co-stained with TRITC-Phalloidin (Life Technologies, OR, USA) and 4′,6-diamidino-2-phenylindole (DAPI, Sigma-Aldrich, USA) for 1 h at room temperature, which could specifically bind with actin filaments (F-actin) and cell nucleus, respectively. The samples were then washed with PBS three times to remove free fluorescent dyes, and the cells in the complexes were photographed with LSCM.

The SHED proliferation on microspheres was confirmed by MTT assay (Sigma-Aldrich). Briefly, the sterilized NF-Ms and PDA-NF-Ms (0.1 mg/well) were respectively placed into 96-well plates to cover the bottom of plate, individually. SHEDs were then seeded onto microspheres in each well at a density of 3×10^3 cells/well. Cells seeded into a 96-well plate directly without microspheres were used as a control group. At the scheduled time points, 20 μl of prepared MTT solution (5 mg/ml) was added into each well and incubated for 3 h at 37 °C. After the resulting supernatant was discarded, 150 μl of dimethyl sulfoxide (DMSO) was then added into per well to dissolve the formazan crystals that formed. The dissolved supernatant was moved to a new 96-well plate and measured by a microplate reader (Bio-Rad 680, USA) at wavelength of 490 nm.

2.7. In vitro osteogenesis study

The bioactivity of the released rhBMP-2 was examined by comparing its ability to induce osteogenic differentiation of BMSCs with that of directly applied rhBMP-2. The osteogenic induction medium components included 50 mg/ml L-ascorbic acid and 10 mM β-glycerol (Sigma, USA). This study contained three groups in total: [1] Blank (BMSCs cultured only with induction medium) group; [2] 100 ng/ml soluble rhBMP-2 group; and [3] rhBMP-2 loaded Hep-Dopa NF-Ms (0.1 mg grafts) group. The extracted medium was collected by incubating 1 mg BMP-2/Hep-Dopa NF-Ms in 10 ml of cultured medium and was refreshed every 2–3 days.

2.7.1. Alkaline phosphatase (ALP) activity

BMSCs were seeded in a 12 well-plate at an initial density of 5×104 cells per well. The induction medium and the medium containing rhBMP-2 was changed every 2–3 days. At days 7 and 14, the BMSCs were fixed with chilled 4% paraformaldehyde for 20 min and rinsed with PBS; subsequently, each group was treated with ALP staining solution (Beyotime, Shanghai, China) for 30 min. The general images were captured using a scanner (HP ScanJet 2400).

In addition, ALP activity was also quantified at the same time points. The cell lysates were prepared by adding 1 ml of distilled water followed by three freeze-thaw cycles. Then, the level of ALP activity was measured using an AKP/ALP assay kit (Jiancheng, Nanjing, China) at an OD_{520nm} and was normalized to the amount of total proteins (BCA assay kit, Biyuntian Biotechnology, China) by using BSA as the standard protein.

2.7.2. Alizarin red S staining (ARS)

When the BMSCs in each group were induced with osteogenic medium for 21 days, the cells were fixed and washed in the same fashion as that used for ALP staining. Furthermore, the solutions were replaced with 1% prepared alizarin red working solution to react with calcium deposits for 20 min and were rinsed with PBS several times. The images were taken using phase contrast microscopy and a scanner.

To quantify the calcium matrix content, the dye was dissolved in 10% cetylpyridinium chloride to release the calcium-bound alizarin red into solution. The absorbance of the supernatant was measured at 562 nm using a microplate reader.

2.7.3. RT-PCR (ALP, Runx2, Coll I)

For RT-PCR assays, BMSCs in each well were rinsed with PBS after 14 days of osteogenic inductive culture, followed by the addition of a 1 ml Trizol reagent (Ambion®, Life Technologies™, USA) to extract the total RNA. The quantity and purity of RNAs were determined at an absorbance at 260/280 nm. Then, cDNA was reverse-transcribed using the PrimeScript® RT reagent Kit (Takara, Japan) according to the manufacturer's protocol. RT-PCR was performed using SYBR Green Master (Roche, USA) via a Step One Plust real-time PCR system (Thermo Fisher, CA). A total of 45 cycles of RT-PCR were carried out and data were normalized to levels of the housekeeper gene β-actin to exclude the influence of cell number. The specific primers of three osteogenic-related genes, including those encoding ALP, Runx2, and Collagen I (Col I), were designed as listed in Table 3.

2.8. In vivo experiments

The osteogenic regenerative capacity of two kinds of modified microspheres and their corresponding composite scaffolds (loading SHED or rhBMP-2) in vivo was determined in ectopic subcutaneous engraftment experiments and an orthotopic cranial bone defect model. All experimental animal procedures were approved by the Animal Care and Use Committee of Peking University (China) in accordance with international standards on animal welfare (authorization number: LA2018001). For the animal surgery, 6–8 weeks old BALB/c nude mice (Weitonglihua Biotechnology, Beijing, China) were anaesthetized by intraperitoneal injection of 4% chloral hydrate (8 ml/kg). A total of 48 nude mice were used and randomly divided into four groups in each animal experiment, and the corresponding groupings and sample abbreviations used in ectopic or orthotopic implantation was listed (see Tables 1 and 2).

2.8.1. Ectopic bone formation upon constructs subcutaneous injection

SHEDs were pre-cultured on PDA-NF-Ms for 7 days to allow for cell proliferation, and this cells/PDA-NF-Ms mixture was then resuspended in medium (in a ratio of 2 mg/ml) prior to implantation. Thereafter, the cells-protein microspheres grafts according to the groups above were injected subcutaneously under the dorsal surface of nude mice (n = 3), respectively. About 1 mg of microspheres or constructs were injected per site, and each mouse accepted two injections of the same group

Table 1
Sample abbreviations used in the ectopic implantation experiment.

Ectopic Implantation	Description of grouping
MS group	PDA-NF-MS and Hep-Dopa NF-Ms (ratio is 1:1)
SHED group	SHED adhered on PDA-NF-MS
BMP-2 group	rhBMP-2 chemically bonded to Hep-Dopa NF-Ms
Dual group	Combination of SHED/PDA-NF-MS and BMP-2/Hep-Dopa NF-Ms (ratio is 1:1)

Table 2
Sample abbreviations used in the orthotopic implantation experiment.

Orthotopic Implantation	Description of grouping
Control group	Empty defect without any filling
SHED group	SHED adhered on PDA-NF-MS
BMP-2 group	rhBMP-2 chemically bonded to Hep-Dopa NF-Ms
Dual group	Combination of SHED/PDA-NF-MS and BMP-2/Hep-Dopa NF-Ms (ratio is 1:1)

which were situated on both sides lateral to the midline. The implants were retrieved at 4 and 8 weeks. At every predetermined time, the transplanted grafts were carefully separated from the surrounding soft tissue. Then, the samples were fixed in 10% neutral formalin and further processed for histologically analysis.

To track the survival time of implanted SHEDs in vivo, the cells had been pre-transfected with green fluorescent protein (GFP)-expression lentiviral (Gene Pharma, Shanghai, China) particles in advance, and stably expressing cell lines were screened by puromycin selection. The mice in the SHED group were sacrificed after 1, 4, or 8 weeks to collect the ectopic explants and detect the GFP-expressing SHED by cryosections. The frozen sections were counterstained with DAPI and further examined using a fluorescent microscope.

2.8.2. *In situ bone regeneration of constructs to repair bone defects*

The ability of co-delivering SHED and rhBMP-2 on NF-Ms to promote orthotopic bone regeneration was measured in a cranial bone defect model. After the mice were anesthetized, a non-healing, full thickness of 4 mm in diameter defect was created in the central region of the cranial bone by using a dental surgical bur. Defects were filled with the prepared SHED/PDA-NF-Ms constructs, rhBMP-2/Hep-Dopa NF-Ms, or their combinations (n = 3). The empty defects without any fillings were served as a control group. The animals were sacrificed at 4 and 8 weeks by injecting a lethal dose of the anesthetic drug into the abdominal cavity. Harvested samples were fixed for at least 24 h for further imaging and histological analysis.

2.8.3. *micro-CT measurement*

At 4 and 8 weeks after implantation, the harvested calvaria bones of all groups were scanned using micro-CT (Skyscan 1076, Bruker, Belgium). After standardized reconstruction using the NR econ software, analysis was carried out using a cylindrical volume of interest with a 4-mm diameter, which was placed over the defected area in the axial plane. Bone volume (BV) and bone mineral density (BMD) of the regenerated tissue were calculated according to the scans reconstructed using the CTAn software (Bruker micro-CT, Belgium).

2.8.4. *Histological analysis*

After CT analysis, the fixed specimens were decalcified in 10% ethylene diamine tetraacetic acid (EDTA) for 7 days, then dehydrated and paraffin-embedded. Sections were cut into 4-mm thick slices and stained by hematoxylin and eosin (H&E) and Masson's trichrome

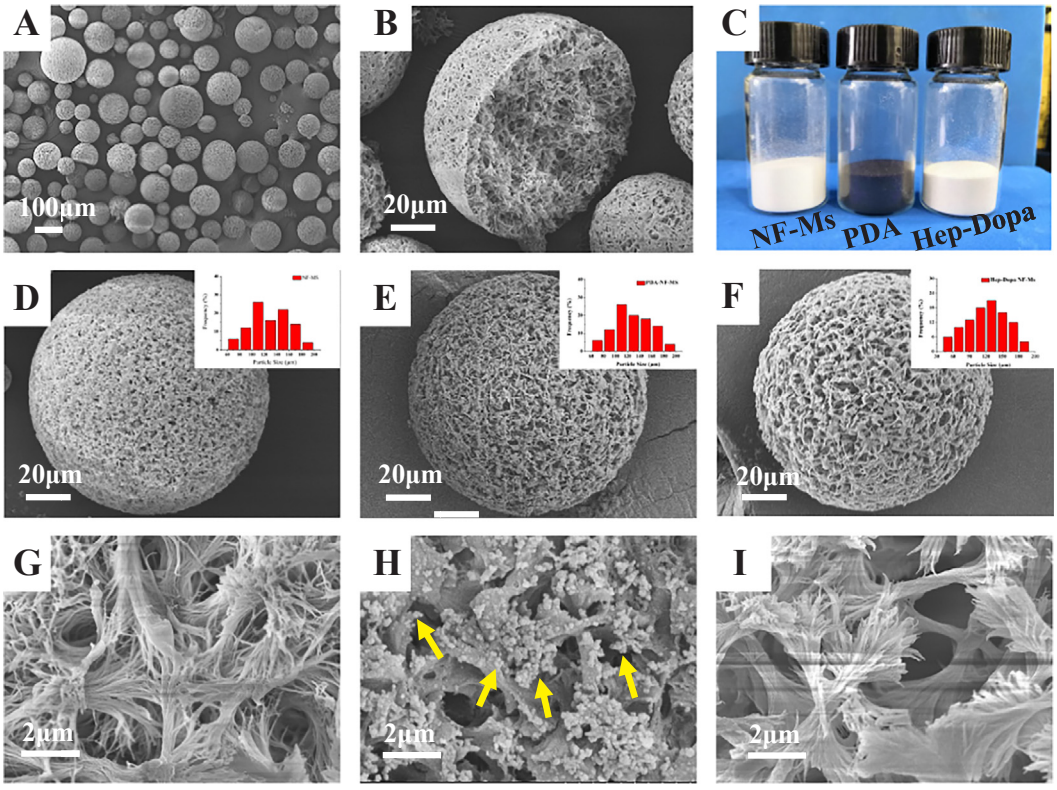

Fig. 1. Morphological characterization and size distribution of various microspheres. Scanning electron microscope images: (A, B, D, G) PLLA NF-Ms (control); (E, H) PDA-NF-Ms; (F, I) Hep-Dopa NF-Ms. (G, H, I) show a local high magnification images of three kinds microspheres, respectively. Yellow arrows indicate PDA aggregates scattered on the surface of NF-Ms. (C) A gross inspection of PLLA NF-Ms with or without surface-modification. The size distribution of various microspheres with a diameter ranging from 50 to 200 μm. (For interpretation of the references to color in this figure legend, the reader is referred to the web version of this article.)

staining (Solarbio, Beijing, China) according to the manufacturer's protocol. The histological staining images were collected with an inverted microscope (Olympus IX-70, NY, America). Then, these images were further measured using Image J software for quantitative assessment of vascular density in new tissues. The number of blood vessels was counted in 5 random fields (×20).

2.9. Statistical analysis

All quantitative data were statistically analyzed through analysis of variance (ANOVA) with Tukey's test, and were expressed as mean ± standard deviation (SD), n ≥ 3. Differences between various groups with $^{*}P < 0.05$ were considered statistically significant and $^{**}P < 0.01$ was considered highly significant.

3. Results

3.1. Characterization of surface-modified PLLA NF-Ms

Visual observation (Fig. 1C) showed that PLLA NF-Ms and Hep-Dopa NF-Ms were white powders, whereas the PDA modified NF-Ms were dark brown-black powders due to the produced by the autoxidation of its monomer dopamine [25].

The morphologies of different PLLA NF-Ms were observed through SEM (Fig. 1A, B, D-I) and the size distribution is presented in Fig. 1(D-F). As shown in the SEM images, the traditional phase separation method gave uniform spheres with an average diameter of the microstructure of ultrafine fibers ranging from 50 to 200 μm. The cross-sectional image in Fig. 1(B) clearly shows the nanofibrous network architecture of PLLA NF-Ms. After the surface was coated with PDA, the diameter of each nanofiber became thicker. In addition, the self-polymerized polydopamine particles were homogeneously scattered on the surface of nanofibers at the nanoscale. Both the PDA-coating and Hep-Dopa decorating modifications made the NF-Ms exhibit a relatively rough surface, but there was no obvious change on spheres size or nanofiber structure.

EDS was used to detect the surface chemical properties of NF-Ms with PDA or Hep-Dopa modifications. Successful PDA or Hep-Dopa immobilization on NF-MS was assessed by the appearance of nitrogen (blue) signals of PDA-NF-MS or nitrogen and sulfur (yellow) signals of

Table 3
Primer sequences of osteogenic-related genes.

Gene name	Primer sequences
β-actin	(Forward)5′CATGTACGTTGCTATCCAGGC-3′ (Reverse) 5′-CTCCTTAATGTCACGCACGAT-3′
ALP	(Forward) 5′-GTGAACCGCAACTGGTACTC-3′ (Reverse) 5′-GAGCTGCGTAGCGATGTCC-3′
Runx2	(Forward) 5′-TGGTTACTGTCATGGCGGGTA-3′ (Forward) 5′-TCTCAGATCGTTGAACCTTGCTA-3′
Coll I	(Forward) 5′-GAGGGCCAAGACGAAGACATC-3′ (Reverse) 5′-CAGATCACGTCATCGCACAAC-3′

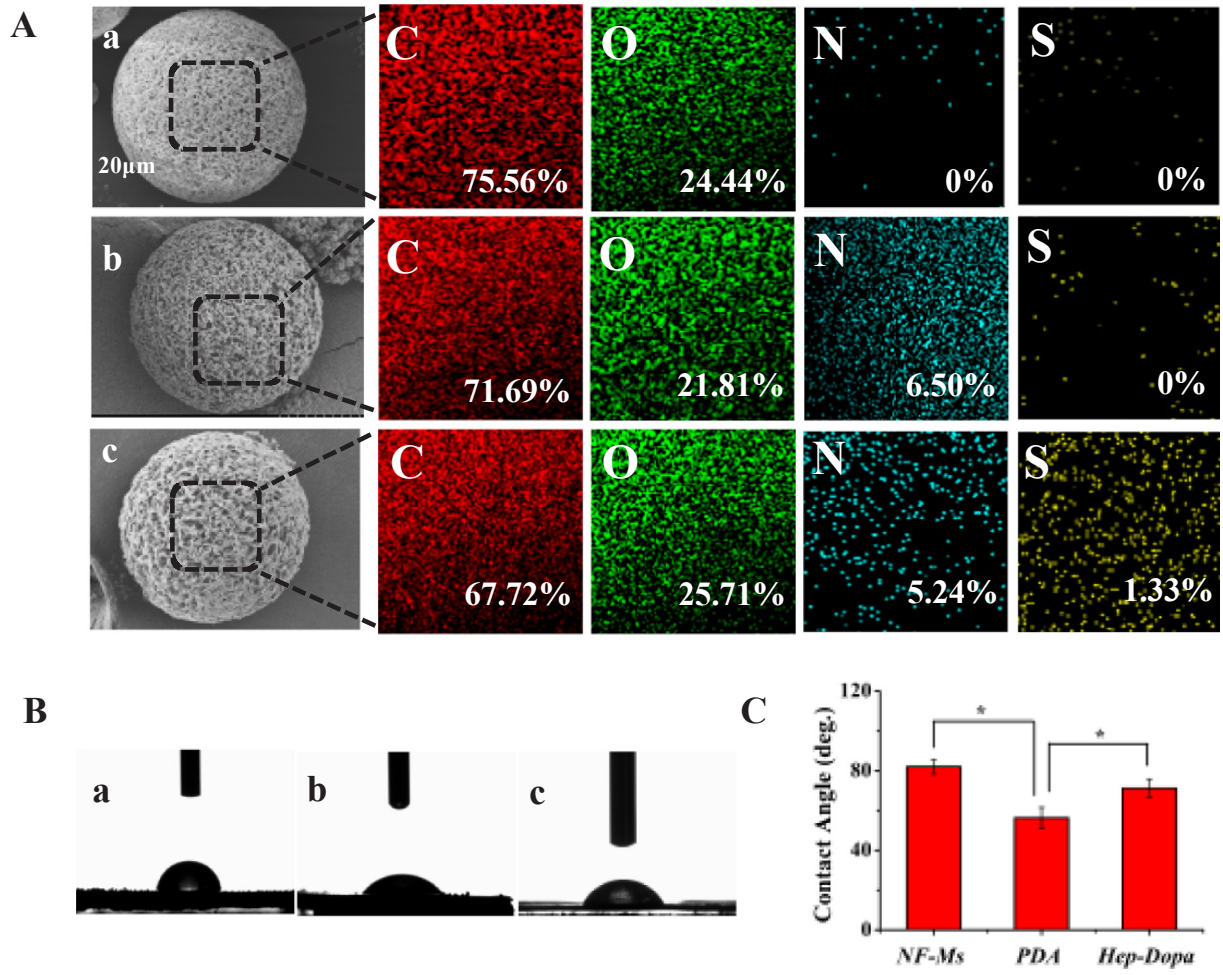

Fig. 2. (A) (A) Mapping images of elemental compositions (including C, O, N, and S elements distribution) of NF-MS by energy dispersive spectroscopy analysis (a), PDA-NF-Ms (b) and Hep-Dopa NF-Ms (c). (B) Water contact angle of (a) PLLA NF-Ms, (b) PDA-modified NF-Ms, and (c) Hep-Dopa NF-Ms. (C) Quantitative results of three kinds of NF-Ms. Statistically analysis by using one-way analysis of variance (ANOVA) ($^{*}P < 0.05$).

Hep-Dopa NF-Ms (Fig. 2A). As further confirmed through EDS analysis (as shown in Table 4), the N1s contents were estimated at 0%, 6.50%, and 5.24%, respectively, and the S2p contents were estimated at 0%, 0%, and 1.33%, respectively.

The apparent WCA was further investigated to evaluate the surface wettability of microspheres after modification with PDA. The surface topography of the scaffold had a great effect on its hydrophilicity; materials possessing nano-/micro- structural morphologies would be especially endowed with high hydrophobicity due to the entrapped air [26]. Hence, these two kinds of NF-Ms were compressed into a regular cylinder to determine the effect of chemical ingredients on the surface properties of these microspheres. As shown in Fig. 2(B and C), the WCA of bare PLLA NF-Ms was about 81.9°. However, the WCA of NF-Ms clearly decreased obviously after the surface modifications of PDA coating or Hep-Dopa conjugation, especially the WCA of PDA-NF-Ms was down to 56.18°.

3.2. Immobilization and release of rhBMP-2 from Hep-Dopa NF-Ms

The distribution of RBITC-labelled rhBMP-2 in microspheres was observed by LSCM. The results shown in Fig. 3(A) were a clear indication that red fluorescence labelled protein was uniformly distributed in Hep-Dopa NF-Ms on each cross section (every 20 μm). In comparison with NF-Ms without modification, the fluorescence intensity also confirmed the effective loading of rhBMP-2 that was integrated with Hep-Dopa onto NF-Ms.

The amount of rhBMP-2 loaded into microspheres was measured by evaluating the difference in weight between the supernatant solutions and loading solutions using an ELISA kit. In contrast to pure PLLA NF-Ms, the loading efficiency of rhBMP-2 in per milligram of Hep-Dopa NF-Ms was remarkably enhanced from 16.7% to 38.2% after decorating with Hep-Dopa (Fig. 3B).

The cumulative release profiles of rhBMP-2 from NF-Ms and Hep-Dopa NF-Ms over a period of 28 days are shown in Fig. 3(C). After NF-Ms being modified with Hep-Dopa conjugation, the initial burst release of rhBMP-2 in 24 h was cut down from 38.02 ± 3.5% to 10.74 ± 2.9%. And the protein release was significantly delayed and displayed a relatively stable release behavior in Hep-Dopa NF-Ms group. After 28 days, approximately 64.93% of the initially loaded rhBMP-2 was released and still kept releasing at a rate of 5.67 ng/day (see SI-Fig. 1).

3.3. Growth and proliferation of SHED on PDA-NF-Ms

Cell morphology was measured by SEM as shown in Fig. 4(A). According to the SEM images, SHED could adhere and spread well both on the NF-Ms both with and without PDA modification. The cells were fully stretched when adhering on PDA-NF-Ms, showing a polygonal morphology with multiple stretched prolongations and extracellular matrix (ECM) on the scaffold surface. Additionally, as shown in the magnified images in Fig. 4(A), SHED extended more pseudopodia between adjacent PDA-NF-Ms which could tightly cling to the surface of microspheres. This observation indicated a better integration of SHED with PDA-NF-Ms than pure NF-Ms.

The viability of SHED cultured on PDA-NF-Ms for 7 days was determined by staining with calcein-AM/PI through LSCM. After the cell and microspheres were co-cultured for 7 days, many green fluorescent SHED could be observed in three-dimensional reconstructed fluorescence images. Moreover, the dead cells labelled with red fluorescence were observed in the PDA-NF-Ms group (Fig. 4B). Cytoskeleton staining suggested that after co-culturing for 7 days, adhered SHED appeared normal, whereas PDA-NF-Ms adopted a stretched shape and formed the cell clusters on the microspheres surfaces.

The proliferation of SHED grown on microspheres was determined by an MTT assay as shown in Fig. 4(C). Both the PLLA NF-Ms and PDA-NF-Ms were conducive to SHED proliferation at different time points. Compared with the control group (TCP, normal tissue culture polystyrene) at 3 days, no significant differences were observed in SHED proliferation between control and PDA-NF-Ms groups. The PDA-NF-Ms gave much higher optical values than the pure NF-Ms group at 3 and 7 days of incubation ($^{*}P < 0.05$ or $^{**}P < 0.01$).

Altogether, our results suggested that the nanofibrous microspheres with PDA surface modifications of PDA were more favorable for SHED growth and proliferation than pure PLLA NF-Ms.

3.4. The osteogenesis effects of rhBMP-2 released from Hep-Dopa NF-Ms

The bioactivity of rhBMP-2 released from Hep-Dopa NF-Ms was assessed through ALP activity, ARS staining, and RT-PCR on BMSCs. Alkaline phosphatase (ALP) is a crucial protein that is produced in the early period of bone formation. As shown in Fig. 5(A), an obvious increase in ALP production by BMSCs in the medium containing rhBMP-2 was confirmed by ALP staining at 7 and 14 days. The relative ALP activity expression of BMSCs was consistently with the staining results as compared with blank group at 7 and 14 days (Fig. 5B) ($^{*}P < 0.05$). In addition, ARS staining and quantification also suggested that groups containing rhBMP-2 exhibited more mineral deposits after sustained induction for 21 days (Fig. 5C and D) ($^{*}P < 0.05$).

The mRNA expression levels of osteogenic differentiation-related genes (ALP, Runx2, and Col1) were analyzed to assess the osteoinductivity of rhBMP-2 for BMSCs at 14 days (Fig. 5E). There was no significant difference in gene expression between the soluble BMP-2 group and the BMP-2/HD NF-Ms group after osteogenic induction for 14 days. However, the expression levels of ALP, Runx2, and Col1 genes in both experimental groups were remarkably up-regulated compared to levels in the blank group, which was only induced by induction medium without bioactive protein at 14 days ($^{*}P < 0.05$ or $^{*}P < 0.01$). This result demonstrated that the rhBMP-2 released from the Hep-Dopa-conjugated microspheres was able to promote BMSCs osteogenic differentiation.

In conclusion, the osteogenic effects of rhBMP-2 obtained from Hep-Dopa NF-Ms was comparable to the effect of 100 ng/ml rhBMP-2 treatment, which proved that the rhBMP-2/HD NF-Ms effectively retained the protein bioactivity effectively and could be potently to induce osteogenic differentiation of BMSCs.

3.5. Ectopic bone formation

The morphology of tissue constructs in various groups at 8 weeks after subcutaneous implantation was shown in Fig. 7(A). The gross appearance of each composited tissue graft exhibited a similar volume, and all the harvested samples remained structurally intact. The white mineralized hard tissues had formed in BMP-2 and Dual groups, whereas the grafts in control and SHED groups were black soft tissue.

3.5.1. Detection of GFP-SHED in vivo

To evaluate the survival situation of SHED growing in explant constructs, cryo-sections of collected samples were processed for histological analysis. From the histological results shown in Fig. 6(A-I), we observed that the GFP-positive SHED (green) were identifiable in the grafts at 7 days (Fig. 6B, C) and 4 weeks (Fig. 6E, F) after implantation in vivo. However, the expression of green fluorescence for implanted

Table 4
Surface elemental compositions of NF-MS, PDA-NF-Ms and Hep-Dopa NF-Ms as determined by EDS analysis.

Samples	C1s%	O1s%	N1s%	S2p%
NF-MS	75.56	24.44	0	0
PDA-NF-MS	71.69	21.81	6.50	0
Hep-Dopa NF-MS	67.72	25.71	5.24	1.33

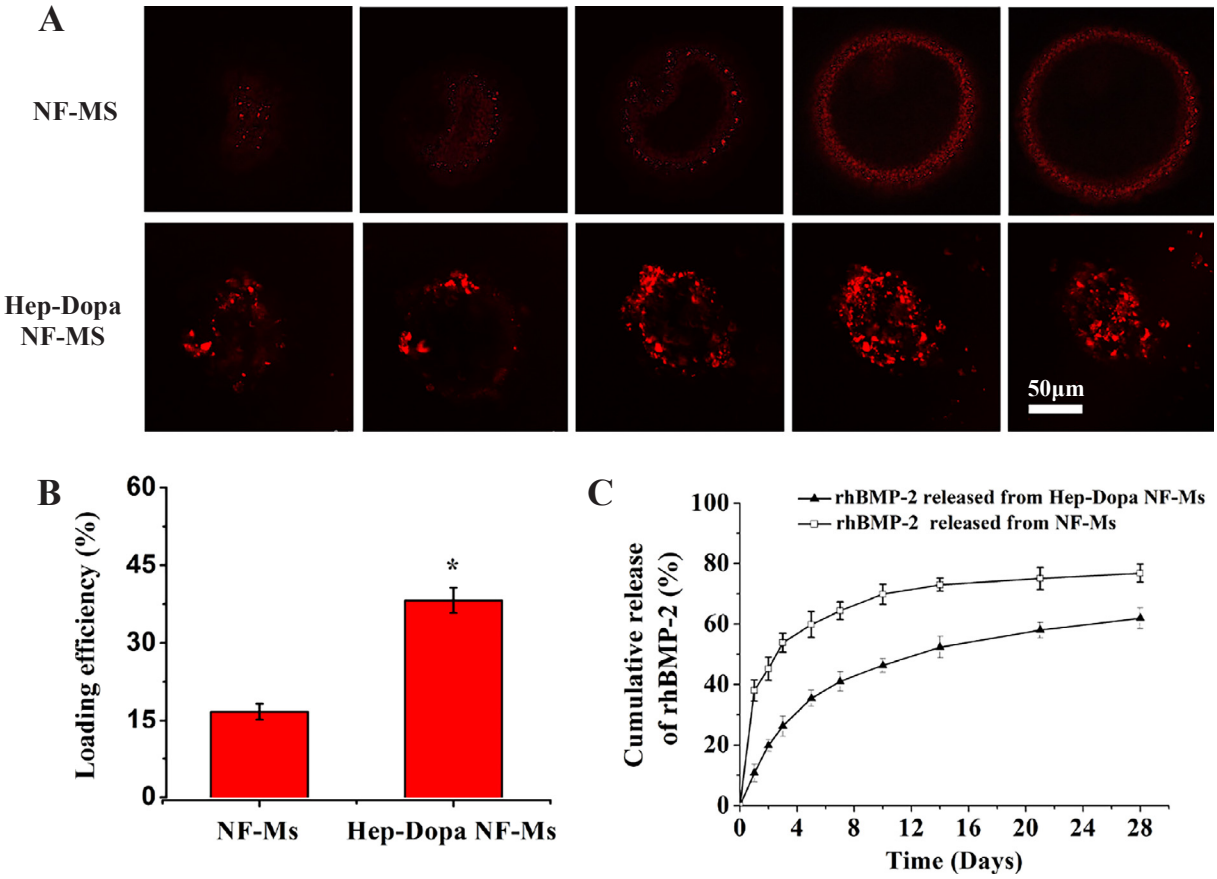

Fig. 3. (A) (LSCM) The distribution of rhBMP-2 in NF-Ms and Hep-Dopa NF-Ms was determined by labelling proteins with red fluorescence. (B) The amount of loaded rhBMP-2 in 1 mg PLLA microspheres (NF-Ms) and 1 mg Hep-Dopa NF-Ms, respectively ($^{*}P < 0.05$). (C) Cumulative release of rhBMP-2 from NF-Ms and Hep-Dopa NF-Ms over a period of 28 days in vitro. Statistically analysis by using one-way analysis of variance (ANOVA) ($^{*}P < 0.05$). (For interpretation of the references to color in this figure legend, the reader is referred to the web version of this article.)

SHED was undetectable at 8 weeks (Fig. 6H, I). All specimens exhibited a large number of infiltrated host cells n (nuclei counterstained with DAPI) at all time points. Our data demonstrated that the implanted SHED had a long-term survival (about 4 weeks) after delivered by PDA-NF-Ms in vivo, which could be contributed in the effective involvement of bone repair process.

3.5.2. Histological observations by H&E and Masson's trichrome staining

As shown in Fig. 7, the PDA-NF-Ms and Hep-Dopa NF-Ms could be distinguished by color differences; the former contained brown microspheres that infiltrated with many cells, and the latter one contained white microspheres that aggregated to form bigger irregular scaffolds (all microspheres are indicated by green arrows). In H&E staining, all cell nuclei were stained in dark blue, the collagenous connective tissues and new bone matrix were highlighted in pink to varying degrees. In contrast to MS group, many neo-vessels formed in the SHED group, filling with abundant hematopoietic cells which were surrounded by SHED-delivered PDA-NF-Ms at 4 and 8 weeks (indicated by red arrows). New bone formation was not detected in these two groups, suggesting that both the modified NF-Ms and SHED could not induce bone regeneration in ectopic sites. Large amounts of interconnected calcified trabecular bones were stained dark blue by Masson's trichrome staining in BMP-2 and Dual groups at predetermined time points. Although the similar bone marrow-like tissues were produced in BMP-2 and Dual groups, however, some adipocytes replaced the bone-marrow like tissues as indicated by asterisks in the BMP-2 group which barely appeared in the Dual group. As described by a previous study, the red-staining osteoid matrixes represents the degree of maturity of bone tissues [27]. At 8 weeks, the Dual group induced the production of a dense reddish blue bone tissue, indicating a greater maturity of regenerated bone tissues compared to that in the BMP-2 group. From the morphology of new bone tissue and quantitative results of vascular density (see Fig. SI-3), we could refer that SHED would function synergistically with rhBMP-2 to improve the quality of neonatal bone during the process of bone regeneration in ectopic location.

3.6. Orthotopic bone regeneration

3.6.1. microCT

The micro-CT images were reconstructed and analyzed to evaluate the 3D structure and amount of the regenerated new bone in an orthotopic bone defect model (Fig. 8A). At 4 and 8 weeks after the operation, new bone had scarcely formed at the defective area in the blank group, presenting a clearly identifiable outline, indicating a rare bone self-healing defect for the 4-mm cranial bone injury in nude mice. Few new bone tissues were produced at the edge of the defect site in SHED groups, while in BMP-2 group, the bulk of generated bone tissues were located from the edge toward the center in the bone defect. However, the newly formed bone volume was much larger in the Dual group than in the other groups, and especially at 8 weeks, the defect area was almost fully covered with new mineralized tissues.

Quantitative analysis was carried out by determining the BV/TV ratios and BMD values within a region of interest based on the micro-CT data. As shown in Fig. 8(B and C), the calculated percentages of BV/TV were consistent with the corresponding BMD values in all groups at 4 and 8 weeks. Interestingly, the SHED group in the orthotopic bone regeneration experiment exhibited osteogenic activity, presenting higher BV/TV (%) and BMD values relative to those in the blank group

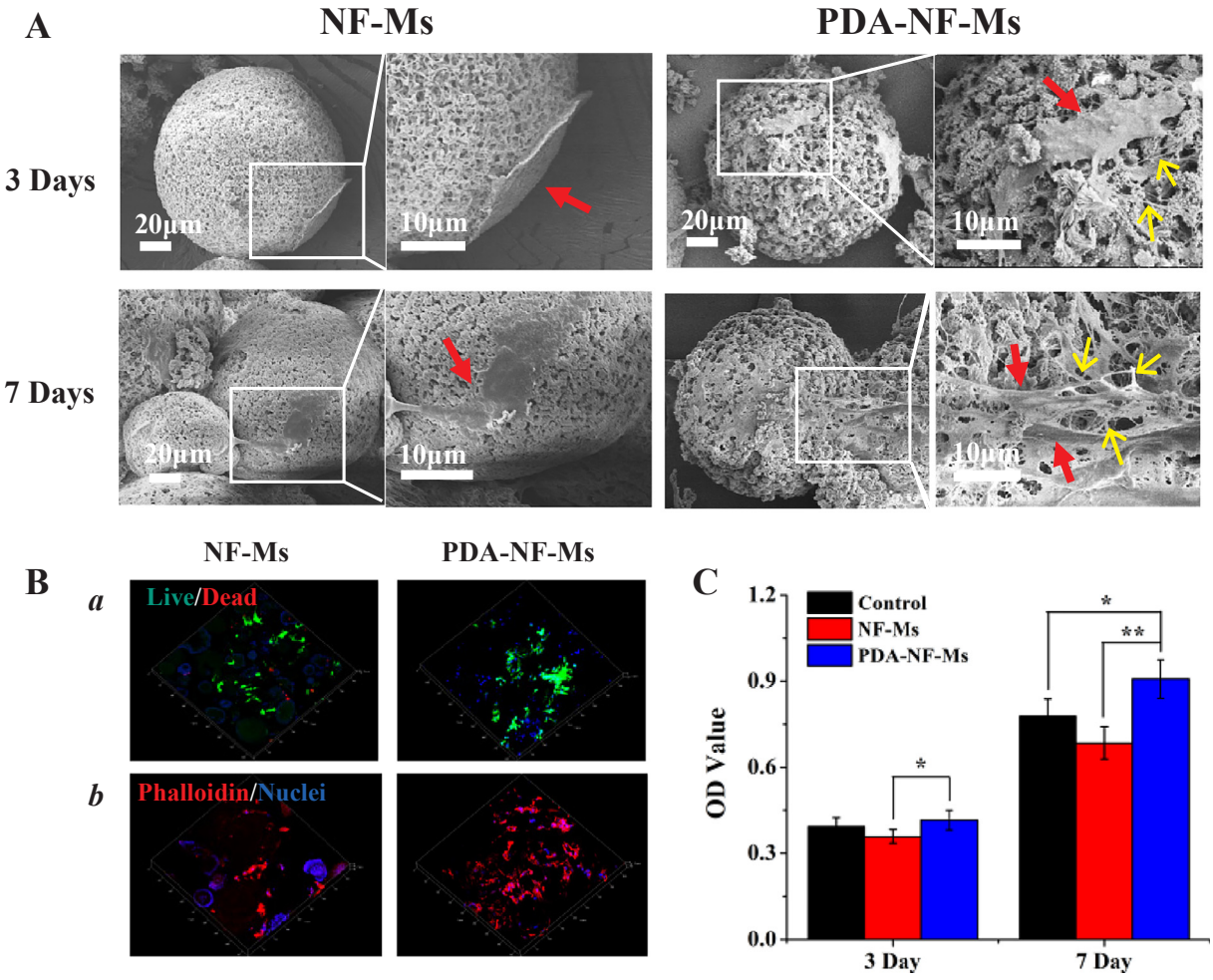

Fig. 4. (A) SEM images: The morphology of cells 3 and 7 days after seeding on NF-Ms and PDA-NF-Ms on 3 days and 7 days. Right panel: high-magnification images of SHEDs adhered on NF-Ms or PDA-NF-Ms for the corresponding white column at different time points (the location of SHED is indicated by red arrows; the ECM is pointed out by yellow arrows). (B) (a) Cell viability staining was performed with calcein AM/PI at 7 days (green representes live cells, red representes dead cells); (b) Observation of cytoskeleton stained with phalloidine (red fluorescence) and nuclei stained with DAPI (blue) of SHEDs on PDA-NF-Ms on 7 days. (C) MTT assay for the SHED proliferation on NF-Ms or PDA-NF-Ms on 3 and 7 days. Statistically analysis by using one-way analysis of variance (ANOVA) ($^{*}P < 0.05$, $^{**}P < 0.01$). (For interpretation of the references to color in this figure legend, the reader is referred to the web version of this article.)

($^{*}P < 0.05$). Although the amount of bone formation in the Dual group was higher than BMP-2 group, no statistically significant difference between these two group. However, both of these two groups were presented potent osteoinductive ability than other groups ($^{*}P < 0.05$ or $^{**}P < 0.01$).

3.6.2. Histological observations by H&E and Masson's trichrome staining

The sagittal sections of calvarial bone were further stained with H&E and Masson's for histological analysis. High-magnification images (200×) were taken to examine vascularization or osteogenesis in all groups. As shown in Fig. 9, a large amount of bone matrix and bone-marrow like structures (as indicated by black arrows) were generated in calvarial defects in the BMP-2 and Dual groups. The conspicuous differences between these two groups was that more red blood cells had infiltrated in the Dual Group at 4 and 8 weeks, with higher vascular density of 1.56 ± 0.59% and 2.53 ± 0.81% respectively (see SI-Fig. 4). In the blank group, there was only a thin-layer of connective tissue had formed in defect area. Meanwhile, a considerable amount of collagenic fibrils deposition (wathet blue) could be observed in the SHED group, and small fragmented tissues were scattered among collagen fibers as pointed out with black arrows (Masson's trichrome staining in Fig. 8D). Furthermore, new vessels dispersed near by the SHED-delivered microspheres (marked with red arrows) in the SHED group. For both 4 and 8 weeks, the new vessels density in SHED group (4 week: 1.59 ± 0.72%; 8 week: 3.48 ± 1.28%) is the highest among all groups ($P < 0.05$). Thus, all above results indicated that SHED/PDA NF-Ms had the potential to induce the angiogenesis and osteogenesis in an orthotopic bone damage environment, and its combination with sustained release of rhBMP-2 by Hep-Dopa NF-Ms contributed to a stronger effect on bone tissue regeneration.

4. Discussion

Recent advances in bone tissue engineering have suggested that biomimetic scaffolds based-stem cells regenerative therapy provides a promising strategy for treating bone defects. However, the performance features of both a scaffold and stem cells have far-reaching effects on bone regeneration outcomes. Therefore, the developed scaffold systems should be continuously optimized and new applications of stem cells should be explored in tissue engineering. The aim of this study was to determine the osteoinductive capacity of SHED supported by PDA-modified PLLA NF-Ms in vivo, and their potential synergy with rhBMP-2, which was slowly released from Hep-Dopa conjugated NF-Ms, in promoting bone regeneration.

Mussel-inspired PDA-coating is readily available via a simple procedure of dopamine (DA) self-polymerization in situ, which has been

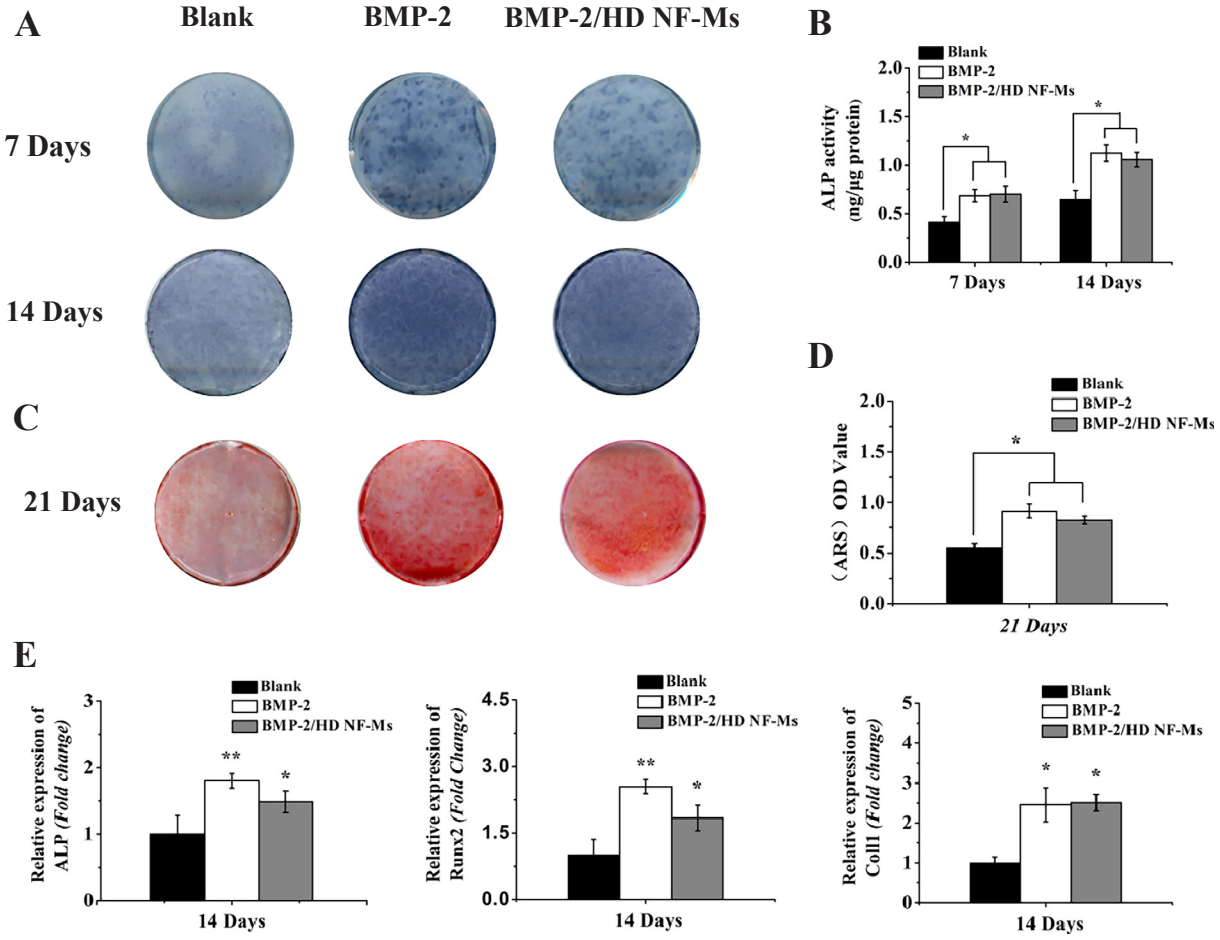

Fig. 5. The osteogenesis effects of 100 ng/ml soluble rhBMP-2 (BMP-2 group) and rhBMP-2 released from Hep-Dopa NF-Ms (BMP-2/HD NF-Ms) on BMSCs in vitro. (A) The ALP staining and (B) quantitative analysis of relative ALP expression on 7 days and 14 days. (C) Alizarin Red S (ARS) staining and (D) quantitative results at the 21st day. (E) Real-time PCR analysis of osteogenic-related gene ALP, Runx2 and Col1 expression of BMSCs in different groups after induced with rhBMP-2 at 14 days. Statistically analysis by using one-way analysis of variance (ANOVA) ($^{*}P < 0.05$, $^{**}P < 0.01$). (For interpretation of the references to color in this figure legend, the reader is referred to the web version of this article.)

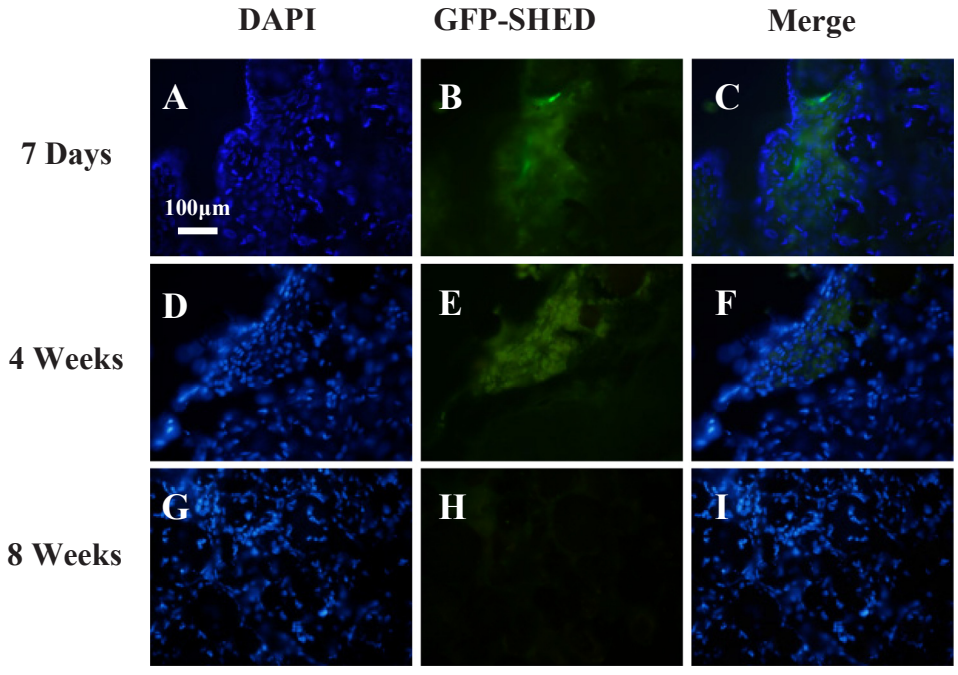

Fig. 6. The survival of SHEDs in the constructs after implantation in vivo at different time points. Fluorescence detection was performed in cryo-sections collected at week 1 (A-C), week 4 (D-F), and week 8 (G-I) after subcutaneous implantation. The GFP-expressing SHED (green; B, E) were observed in ectopic tissue grafts at 1 and 4 weeks, but undetectable at 8 weeks (H). Scale bars (A-I): 100 μm. (For interpretation of the references to color in this figure legend, the reader is referred to the web version of this article.)

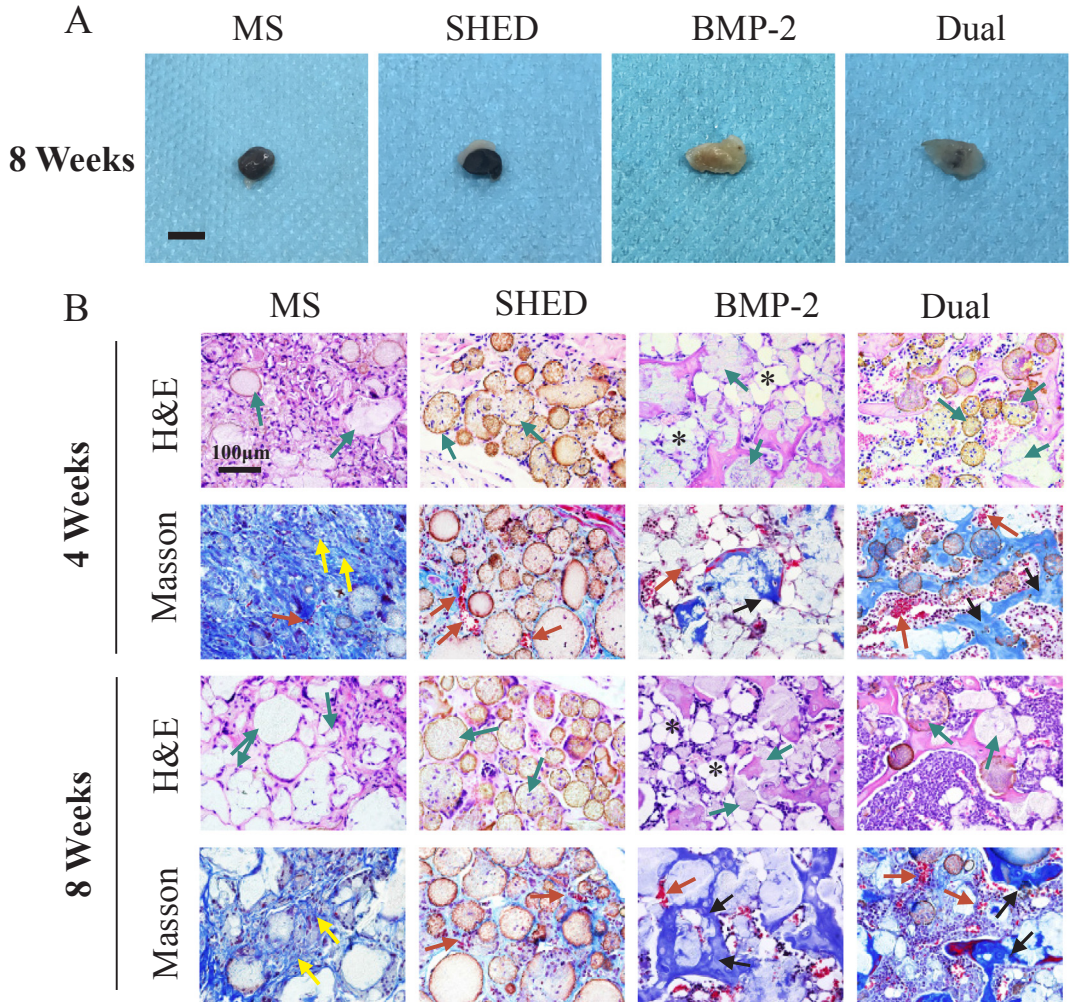

Fig. 7. The new bone tissue formation of ectopic implants in various groups. (A) Gross appearance of tissue constructs of each group at 8 weeks. (B) Histological examination of ectopic implants was carried out at 4 and 8 weeks, and all representative samples were stained with H&E staining and Masson's trichrome staining. Asterisks mark the location of adipocytes in bone marrow-like tissues. (Yellow arrows denoted connective tissue. Green arrows denoted the residual microspheres for each group. Red arrows denote the newly formed vessels around the microspheres and black arrows denote the nascent bone matrix). (For interpretation of the references to color in this figure legend, the reader is referred to the web version of this article.)

introduced to improve cellular attachment on tissue engineering scaffolds [18,28]. Yang et al. reported that surface functionalization of PLA-composited scaffolds through PDA coating could effectively improve the hydrophilicity and biocompatibility of polymer-based scaffolds [29]. Inspired by those characteristics of PDA-assisted modification, we successfully prepared an injectable PDA-NF-Ms to improve the

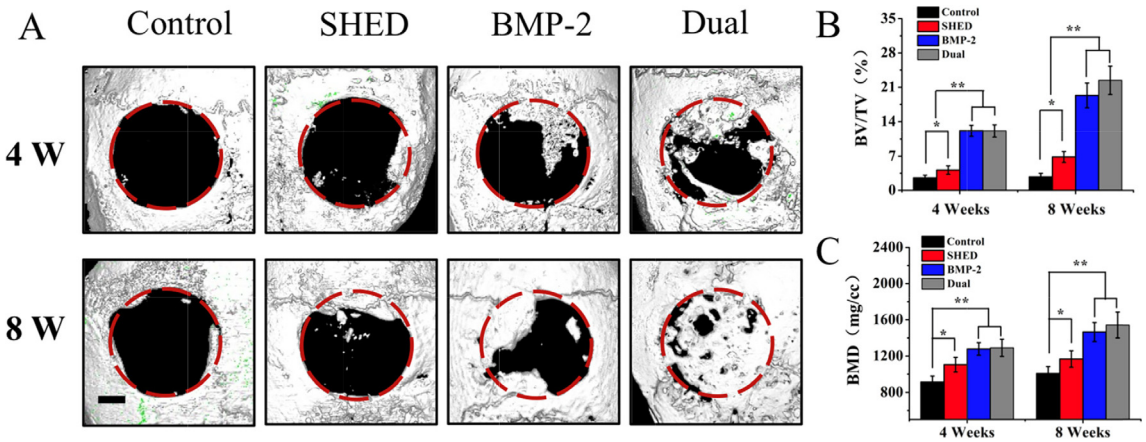

Fig. 8. (A) Reconstructive 3D micro-CT photographs of repaired cranial bone defects in all groups at 4 and 8 weeks post-operation (scale bar: 1 mm) in nude mice (n = 3). (B) Quantitative analysis of BV/TV, and (C) BMD values for four groups. Statistically analysis by using one-way analysis of variance (ANOVA) ($^{*}P < 0.05$, $^{**}P < 0.01$).

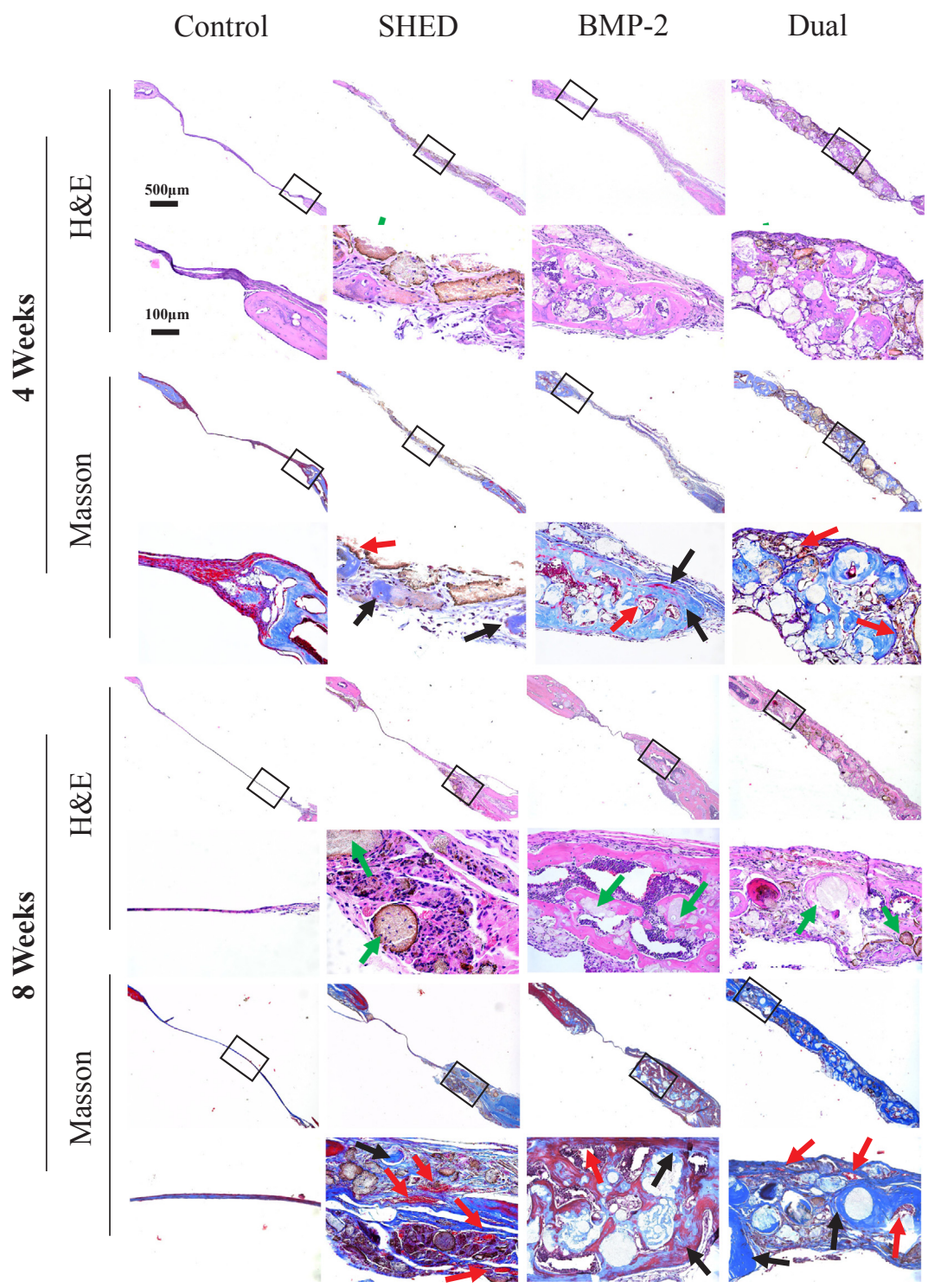

Fig. 9. Histological analysis by H&E staining and Masson's trichrome staining of different construct groups after implantation at 4 and 8 weeks (at 40× and at 200×). Green arrows showed the remnant microspheres. Red arrows denoted new blood vessels. Black arrows pointed to the ossification center and nascent bone matrix in each group. (For interpretation of the references to color in this figure legend, the reader is referred to the web version of this article.)

biological property of PLLA NF-Ms. As a synthetic simulant of naturally produced melanin [30], PDA is an insoluble brown-black particulate that changes the original color of the scaffold (Fig. 1C). SEM images showed the nanometer-sized PDA particles were homogeneously scattered on the fiber surface of microspheres with an average diameter about 100 μm (Fig. 1H). Furthermore, the WCA results revealed a great increase in the hydrophilicity of PLA NF-Ms after modification with PDA coating (Fig. 2B), exhibiting desired properties of a scaffold to support cell adhesion and stretching [18].

The cellular growth behavior influenced by a scaffold surface is an important parameter to evaluate the biological properties of a scaffold material [31,32]. As we expected, the number of SHED sticking on the surface of PDA-NF-Ms was greater than the number of unmodified PLA microspheres. Remarkably, the adhered SHED secreted a plenty of extracellular matrix (ECM) for cell-materials connections, which might be due to the increased roughness imparted by PDA particles and the ECM-

like architecture (Fig. 4A) [33]. Proliferation assay results also supported the observed results that the PDA-NF-Ms boosted SHED expansion in comparison with monolayer tissue plates or bare NF-Ms. Another explanation for the enhanced cellular adhesion and proliferation observed on the PDA layer is the potent reactivity of PDA to other nucleophiles [25], and the leached DA monomers promotes cell attachment via integrin signaling [18].

Additionally, the functional groups of DA (such as catechol and amine) can easily react with heparin and form Hep-Dopa conjugation. Such conjugation improves the covalent immobilization of serum adhesive proteins onto scaffolds surfaces, which promotes controlled release [34,35]. To fabricate efficient injectable microspheres to sustain release protein, Hep-Dopa conjugation was first introduced into PLA NF-Ms systems. Due to the strongly electrostatic interactions between heparin and proteins [35], functionalized Hep-Dopa NF-Ms showed increased rhBMP-2 immobilization and sustained release over 28 days without an initial sudden release trend, which possessed distinguished advantages over the neat PLA-NF-Ms. NF-Ms was not widely studied in the application of protein delivery system currently. According to the previous report, a hierarchical nanofibrous PLLA microspheres has been successfully prepared for protein sustained release, which was realized by encapsulating the gelatin nanospheres into PLA NF-Ms [37]. Based on that, our design of Hep-Dopa NF-Ms provided an optional strategy to serve as an injectable protein delivery system in a more simple and efficient way.

As a major component of the bone marrow niche, MSCs possess the ability to give rise to other committed lineages to maintain the balance of bone remolding [36]. Therefore, we evaluated the osteogenesis of BMSCs to verify the bioactivity of released rhBMP-2 compared to the direct application of soluble rhBMP-2. As proved by results, the soaked medium collecting from protein-loaded microspheres had a similar stimulatory effect on promoting BMSCs osteogenic differentiation (Fig. 5A–E), indicating the retained bioactivity and effective osteoinductivity of rhBMP-2 released from Hep-Dopa NF-Ms. In natural ECM, heparin has a high affinity for proteins, providing the binding domain. Herein, heparin served as a reservoir for rhBMP-2 and immobilized onto NF-Ms surface with the conjugation of DA to maintain its long-term bioactivity [37].

The ectopic subcutaneous implantation of cell carriers has helped assess the biological properties of the scaffold and define the multipotent functions of grafted cells [36]. The previous study demonstrated that PDA cannot mobilize stem cells into wounded sites [38]. And our ectopic results also suggested the modified PLA NF-Ms (with surface modification of PDA or Hep-Dopa) did not show the inducibility on promoting angiogenesis or osteogenesis in ectopic site (Fig. 7B). Yao et al. also revealed that modifications with both dopamine and Hep-Dopa slightly affected the osteogenic differentiation, which can be neglected [34]. As a result, we removed the modified NF-Ms (control) group in the follow-up orthotopic cranial defect experiment to avoid unnecessary animal sacrifices in consideration of animal ethics.

Federico et al. profiled the secretome of SHED and found a high production of specific bioactive factors (like stromal cell-derived factor-1α (SDF-1α) and hepatocyte growth factor (HGF), which play an essential role in mobilizing endogenous progenitor cells and maintaining cell survival to activate tissue repairing pathways [39]. Accordingly, in our in vivo experiment, SHED which delivered by PDA-NF-Ms were not only alive for more than 4 weeks after transplantation in vivo (Fig. 6), but also presented a pronounced pro-angiogenesis behavior compared to other groups. Nevertheless, orthotopically implanted SHED by PDA-NF-Ms into the defect area showed a sign of new bone matrix deposition accompanied with capillary invasions (Fig. 8A, D), while the ectopic site merely exhibited neo-vessels without ossification potential (Fig. 7B). This discrepancy might be explained by variations in the microenvironment. In such a subcutaneous ectopic bone formation model, the shortage of growth factors and osteoprogenitor cells surrounding the implanted grafts could hardly trigger the bone signaling cascades [40]. Thus, it is more difficult to regenerate bone tissues in a subdermal environment than in an orthotopic bone defect, in which the transplanted cells can indirectly contact local MSCs for cellular communication [41]. As a prominent osteogenic activator, the effectiveness of rhBMP-2 that was delivered sustainably via Hep-Dopa NF-Ms and its potential additional effects on bone regeneration in combination with SHED/PDA-NF-Ms were also determined at ectopic and orthotopic sites. Unlike SHED grafts, the osteoinductivity of the rhBMP-2/Hep-Dopa NF-Ms composited scaffold was similar between the two different experimental models. New bone formation was clearly enhanced in all groups with rhBMP-2 within 4 and 8 weeks' post-implantation, as determined by micro-CT analysis and histological observation both in ectopic and orthotopic sites (Fig. 7B and Fig. 8). More vascularized new bone tissues were deposited in the Dual group than upon application of rhBMP-2/Hep-Dopa NF-Ms constructs alone. This result revealed the positive effect of SHED on improving bone tissue regeneration outcomes in synergy with rhBMP-2. However, the issues of the final SHED destination after 4 weeks implantation, and the mechanisms underlying the synergistic effect of SHED and bioactive factors need to be clarified in further studies.

5. Conclusion

The results of the present signify that the bioinspired surface modification with PDA could endow the PLLA NF-Ms scaffold with good cell affinity, providing a better living space to support SHED adhesion, proliferation, and viability. Meanwhile, PLLA NF-Ms can be used to load high amounts of bioactive rhBMP-2 after modification with Hep-Dopa, achieving the on-demand controlled release of the protein to elicit a functional cellular response in vitro and in vivo. Consequently, the modified scaffold can specifically provide a versatile platform for the effective delivery of stem cells and growth factors. SHED cannot directly differentiate into osteoblast-lineage cells without induction by growth factors in vivo. However, SHED mediated the early vascularization process, largely via its potential paracrine trophic effect to promote MSC recruitment, and the interactions between grafted SHED and the host microenvironment could further influence the outcome of bone tissue regeneration. Taken together, the involvement of SHED contributes to the angiogenesis process as a prerequisite for regenerating vascularized bone tissue, and this novel strategy, which specifically delivers SHED and rhBMP-2 via a modified injectable NF-Ms scaffold, is promising for bone tissue engineering.

Conflict of interests

The authors declare no conflicting financial or other competing interests in this research.

Funding statement

This work was supported by grants from the National Natural Science Foundation of China (303076129, 51873018) and the Stomatology Development Fund of Tason.

Appendix A. Supplementary data

Supplementary data to this article can be found online at https://doi.org/10.1016/j.cej.2019.03.151.

References

[1] P. Lichte, H.C. Pape, T. Pufe, P. Kobbe, H. Fischer, Scaffolds for bone healing: concepts, materials and evidence, Injury 42 (2011) 569–573.
[2] Z. Buser, D.S. Brodke, J.A. Youssef, H.J. Meisel, S.L. Myhre, R. Hashimoto, J.B. Park, S. Tim Yoon, J.C. Wang, Synthetic bone graft versus autograft or allograft for spinal fusion: a systematic review, J. Neurosurg. Spine 25 (2016) 509–516.
[3] A.M. Yousefi, P.F. James, R. Akbarzadeh, A. Subramanian, C. Flavin, H. Oudadesse,

Prospect of stem cells in bone tissue engineering: a review, Stem. Cells. Int 10 (2016) 6180487.
[4] M.R. Todeschi, R. El Backly, C. Capelli, A. Daga, E. Patrone, M. Introna, R. Cancedda, M. Mastrogiacomo, Transplanted umbilical cord mesenchymal stem cells modify the in vivo microenvironment enhancing angiogenesis and leading to bone regeneration, Stem. Cells. Dev. 24 (2015) 1570–1581.
[5] B.M. Seo, W. Sonoyama, T. Yamaza, C. Coppe, T. Kikuiri, K. Akiyama, J.S. Lee, S. Shi, SHED repair critical-size calvarial defects in mice, Oral. Dis. 14 (2010) 428–434.
[6] S. Annibali, M.P. Cristalli, F. Tonoli, A. Polimeni, Stem cells derived from human exfoliated deciduous teeth: a narrative synthesis of literature, Eur. Rev. Med. Pharmacol. Sci. 18 (2014) 2863–2881.
[7] G.T. Huang, S. Gronthos, S. Shi, Mesenchymal stem cells derived from dental tissues vs. those from other sources: their biology and role in regenerative medicine, J. Dent. Res. 88 (2009) 792–806.
[8] J. Ishikawa, N. Takahashi, T. Matsumoto, Y. Yoshioka, N. Yamamoto, M. Nishikawa, H. Hibi, N. Ishigro, M. Ueda, K. Furukawa, A. Yamamoto, Factors secreted from dental pulp stem cells show multifaceted benefits for treating experimental rheumatoid arthritis, Bone 83 (2016) 210–219.
[9] Y. Nishino, Y. Yamada, K. Ebisawa, S. Nakamura, K. Okabe, E. Umemura, K. Hara, M. Ueda, Stem cells from human exfoliated deciduous teeth (SHED) enhance wound healing and the possibility of novel cell therapy, Cytotherapy 13 (2011) 598–605.
[10] T. Inoue, M. Sugiyama, H. Hattori, H. Wakita, T. Wakabayashi, M. Ueda, Stem cells from human exfoliated deciduous tooth-derived conditioned medium enhance recovery of focal cerebral ischemia in rats, Tissue. Eng. Part. A 19 (2013) 24–29.
[11] X. Liu, P.X. Ma, Polymeric scaffolds for bone tissue engineering, Ann. Biomed. Eng. 32 (2004) 477–486.
[12] J. Fang, Y. Zhang, S. Yan, Z. Liu, S. He, L. Cui, J. Yin, Poly(L-glutamic acid)/chitosan polyelectrolyte complex porous microspheres as cell microcarriers for cartilage regeneration, Acta. Biomater. 10 (2014) 276–288.
[13] M.B. Dreifke, N.A. Ebraheim, A.C. Jayasuriya, Investigation of potential injectable polymeric biomaterials for bone regeneration, J. Biomed. Mater. Res. A 101 (2013) 2436–2437.
[14] C. Bei, N. Ahuja, M. Chi, X. Liu, Injectable scaffolds: preparation and application in dental and craniofacial regeneration, Mater. Sci. Eng. R. Rep. 111 (2017) 1–26.
[15] R. Kuang, Z. Zhang, X. Jin, J. Hu, S. Shi, L. Ni, P.X. Ma, Nanofibrous spongy microspheres for the delivery of hypoxia-primed human dental pulp stem cells to regenerate vascularized dental pulp, Acta Biomater. 33 (2016) 225–234.
[16] S. Chen, B. Bai, D.J. Lee, S. Diachina, Y. Li, S.W. Wong, Z. Wang, H.C. Tseng, C.C. Ko, Dopaminergic enhancement of cellular adhesion in bone marrow derived mesenchymal stem cells (MSCs), J. Stem. Cell. Res. Ther. 7 (2017) 395.
[17] J.D. Boerckel, Y.M. Kolambkar, K.M. Dupont, B.A. Uhrig, E.A. Phelps, H.Y. Stevens, A.J. García, R.E. Guldberg, Effects of protein dose and delivery system on BMP-mediated bone regeneration, Biomaterials 32 (2011) 5241–5251.
[18] Z. Zheng, W. Yin, J.N. Zara, W. Li, J. Kwak, R. Mamidi, M. Lee, R.K. Siu, R. Ngo, J. Wang, D. Carpenter, X. Zhang, B. Wu, K. Ting, C. Soo, The use of BMP-2 coupled – nanosilver-PLGA composite grafts to induce bone repair in grossly infected segmental defects, Biomaterials 31 (2010) 9293–9300.
[19] Y. Takahashi, M. Yamamoto, Y. Tabata, Enhanced osteoinduction by controlled release of bone morphogenetic protein-2 from biodegradable sponge composed of gelatin and β -tricalcium phosphate, Biomaterials 26 (2005) 4856–4865.
[20] J. Zhou, X. Guo, Q. Zheng, Y. Wu, F. Cui, B. Wu, Improving osteogenesis of three-dimensional porous scaffold based on mineralized recombinant human-like collagen via mussel-inspired polydopamine and effective immobilization of BMP-2-derived peptide, Colloids Surf. B. Biointerfaces 152 (2017) 124–132.
[21] M.H. Hettiaratchi, T. Miller, J.S. Temenoff, R.E. Guldberg, T.C. McDevitt, Heparin microparticle effects on presentation and bioactivity of bone morphogenetic protein-2, Biomaterials 35 (2014) 7228–7238.
[22] S.E. Kim, Y.P. Yun, K.S. Shim, K. Park, S.W. Choi, D.H. Shin, D.H. Suh, Fabrication of a BMP-2-immobilized porous microsphere modified by heparin for bone tissue engineering, Colloids Surf. B. Biointerfaces 134 (2015) 453–460.
[23] X. Liu, X. Jin, P.X. Ma, Nanofibrous hollow microspheres self-assembled from star-shaped polymers as injectable cell carriers for knee repair, Nat. Mater. 10 (2011) 398–406.
[24] Z. Wang, K. Wang, X. Lu, M. Li, H. Liu, C. Xie, F. Meng, O. Jiang, C. Li, W. Zhi, BMP-2 encapsulated polysaccharide nanoparticle modified biphasic calcium phosphate scaffolds for bone tissue regeneration, J. Biomed. Mater. Res. A 103 (2015) 1520–1532.
[25] R. Batul, T. Tamanna, A. Khaliq, A. Yu, Recent progress in the biomedical applications of polydopamine nanostructures, Biomater. Sci. 5 (2017) 1204–1229.
[26] W. Zhang, M. Liu, Y. Liu, R. Liu, F. Wei, R. Xiao, H. Liu, 3D porous poly (L-lactic acid) foams composed of nanofibers, nanofibrous microsheaves and microspheres and their application in oil–water separation, J. Mater. Chem. A 3 (2015) 14054–14062.
[27] B. Zhang, H. Li, L. He, Z. Han, T. Zhou, W. Zhi, X. Lu, X. Lu, J. Weng, Surface-decorated hydroxyapatite scaffold with on-demand delivery of dexamethasone and stromal cell derived factor-1 for enhanced osteogenesis, Mater. Sci. Eng. C. Mater. Biol. Appl. 89 (2018) 355–370.
[28] W. Yang, X. Zhang, K. Wu, X. Liu, Y. Jiao, C. Zhou, Improving cytoactive of endothelial cell by introducing fibronectin to the surface of poly L-Lactic acid fiber mats via dopamine, Mater. Sci. Eng. C. Mater. Biol. Appl. 69 (2016) 373–379.
[29] Z. Yang, J. Si, Z. Cui, J. Ye, X. Wang, Q. Wang, K. Peng, W. Chen, S.C. Chen, Biomimetic composite scaffolds based on surface modification of polydopamine on electrospun poly (lactic acid)/cellulose nanofibrils, Carbohydr. Polym. 174 (2017) 750–759.
[30] B.P. Tripathi, N.C. Dubey, R. Subair, S. Choudhurya, M. Stammab, Enhanced hydrophilic and antifouling polyacrylonitrile membrane with polydopamine modified silica nanoparticles, RSC. Adv. 6 (2016) 4448–4457.
[31] L. Ghasemi-Mobarakeh, M.P. Prabhakaran, L. Tian, E. Shamirzaei-Jeshvaghani, L. Dehghani, S. Ramakrishna, Structural properties of scaffolds: crucial parameters towards stem cells differentiation, World. J. Stem. Cells. 7 (2015) 728–744.
[32] G. Zhao, A.L. Raines, M. Wieland, Z. Schwartz, B.D. Boyan, Requirement for both micron- and submicron scale structure for synergistic responses of osteoblasts to substrate surface energy and topography, Biomaterials 28 (2007) 2821–2829.
[33] B.N. Teixeira, P. Aprile, R.H. Mendonça, D.J. Kelly, R.M.D.S.M. Thiré, Evaluation of bone marrow stem cell response to PLA scaffolds manufactured by 3D printing and coated with polydopamine and type I collagen, J. Biomed. Mater. Res. B. Appl. Biomater. (2018) [Epub ahead of print].
[34] Q. Yao, Y. Liu, H. Sun, Heparin-dopamine functionalized graphene foam for sustained release of bone morphogenetic protein-2, J. Tissue. Eng. Regen. Med. 12 (2018) 1519–1529.
[35] S.E. Kim, Y.P. Yun, K.S. Shim, K. Park, S.W. Choi, D.H. Suh, Effect of lactoferrin-impregnated porous poly(lactide-co-glycolide) (PLGA) microspheres on osteogenic differentiation of rabbit adipose-derived stem cells (rADSCs), Colloids Surf. B. Biointerfaces 122 (2014) 457–464.
[36] A. Abarrategi, S.A. Mian, D. Passaro, K. Rouault-Pierre, W. Grey, D. Bonnet, Modeling the human bone marrow niche in mice: from host bone marrow engraftment to bioengineering approaches, J. Exp. Med. 215 (2018) 729–743.
[37] X. Li, C. Ma, X. Xie, H. Sun, X. Liu, Pulp regeneration in a full-length human tooth root using a hierarchical nanofibrous microsphere system, Acta. Biomater. 35 (2016) 57–67.
[38] Saurav Shome, Partha Sarathi Dasgupta, Sujit Basu, Dopamine regulates mobilization of mesenchymal stem cells during wound angiogenesis, Plos One 7 (2012) e31682.
[39] F. Mussano, T. Genova, S. Petrillo, I. Roato, R. Ferracini, L. Munaron, Osteogenic differentiation modulates the cytokine, chemokine, and growth factor profile of ASCs and SHED, Int. J. Mol. Sci. 19 (2018) E1454.
[40] M.A. Scott, B. Levi, A. Askarinam, A. Nguyen, T. Rackohn, K. Ting, C. Soo, A.W. James, Brief review of models of ectopic bone formation, Stem. Cells. Dev. 21 (2012) 655–667.
[41] C.H. Lee, M.U. Jin, H.M. Jung, J.T. Lee, T.G. Kwon, Effect of dual treatment with SDF-1 and BMP-2 on ectopic and orthotopic bone formation, PLoS. One 10 (2015) e0120051.